Robotic Scanning Absorption Spectroscopy for Methane Leak Detection: the Virtual Gas Camera

Heiko Lohrke, Harald Kohlhoff, Patrick P. Neumann
Bundesanstalt für Materialforschung und -prüfung (BAM), Berlin, Germany
heiko.lohrke@bam.de

Abstract—This paper explores combining a gimbal-mounted tunable diode laser absorption spectroscopy (TDLAS) sensor and a video camera to create a virtual gas camera for methane leak detection. This provides a low-to-zero-cost extension of typical TDLAS gas tomography systems. A prototype setup mounted on a ground robot is evaluated. Results acquired using a simulated methane leak show the feasibility of the virtual gas camera, accurately detecting methane leaks by overlaying concentrations onto a visual image. While the acquisition time is significantly longer than for traditional gas cameras, potential enhancements are discussed. The study concludes that the virtual gas camera is feasible and useful, despite its longer acquisition time. It serves as a valuable software-only addition to typical TDLAS gas tomography systems, offering quickly-available on-site data augmentation for visual leak assessment at low-to-zero cost.

I. Introduction

Methane, a combustible and potent greenhouse gas, necessitates prompt detection in industrial areas and landfills to prevent hazards and environmental issues [1], [2].

For detection of methane, multiple technologies are available. Of particular interest for this paper are gas cameras (optical gas imaging, OGI) and tunable diode laser absorption spectroscopy (TDLAS). Their main difference is that while gas cameras visually show gas absorption in their field of view, TDLAS measures the integral absorption along a laser beam.

Gas cameras allow for straightforward analysis of leaks. This is because they display a visual image where plumes of gas will simply appear as dark or bright clouds. This is either due to their absorption at the IR operating wavelength or an (apparent) temperature difference of gas vs. background [3]. A consequence of this is a very intuitive gas visualization. Yet, common gas cameras have difficulties in estimating the absolute amount of gas along the line of sight and suffer from cross-sensitivity to other gases [4].

TDLAS, on the other hand, has more of a pinpoint characteristic. It detects methane presence by measuring the attenuation of a laser beam tuned to an absorption line of methane. Usually, the detector is integrated into the device and a surface in the area of interest is used as a diffuse reflector. To correct for different amounts of returned light, measurements are simultaneously performed at a reference wavelength where methane does not absorb. From this, the absolute integrated concentration along the laser path or column density can be calculated [5]. This quantity is usually expressed as product of ppm and meter (ppm·m). Such measurements do not have the intuitive overview characteristic of a gas camera. Yet, they allow for precise column density quantification due to the reference measurement and are very gas-specific.

With gas tomography, TDLAS can be extended to produce 2D slices similar to medical computer tomography (CT). For this, the TDLAS system is mounted on a pan/tilt unit or gimbal, and measurement sweeps from multiple locations and angles are acquired. Tomographic reconstruction algorithms are then employed to arrive at horizontal 2D slices of the gas concentration in the analyzed area. [2], [6], [7]

A minimal TDLAS setup can thus only be used in pinpoint mode. Alternatively, if gas tomography is employed, it will require multiple measurement locations, as well as a longer acquisition time [2], [6], [7]. This is not compatible with a real-time leak investigation as could be performed by gas cameras. It furthermore does not directly correlate to visual information.

However, many systems used for TDLAS measurements also incorporate a video camera [1], [7]. It is therefore conceivable to use this information in connection with the pan/tilt unit or gimbal, to acquire visual and methane presence information simultaneously. Transformed into a suitable presentation, this would allow a typical TDLAS gas tomography setup to act as a virtual gas camera. Such a system would need to acquire the visual information matching a specific angle (referred to in this work as a subframe) and TDLAS measurements over the original field of view of the camera. Afterwards, this data can be assembled into a visual representation of the leaking gas. This would essentially add a second virtual gas camera operational mode to the TDLAS system at no or little additional hardware cost.

Previous work has already performed sweeps to determine gas concentrations across an area of interest [1], [2], [6], [7]. Yet, none of it has directly correlated measured methane concentrations with video frame visual data in the fashion outlined above.

The main question that this paper seeks to answer is thus if a system consisting of an open-path TDLAS sensor mounted on a gimbal can indeed be used as a virtual gas camera. To be more specific, the question is if (methane) gas leak detection can be performed, and a visual assessment of a location is possible. In connection with this, the goal is also to present a prototype system for this concept and evaluate its performance. A secondary goal is to present the findings and pitfalls identified, and publish the developed setup and software. This contribution would allow others to also extend their TDLAS setups with a virtual gas camera simply by
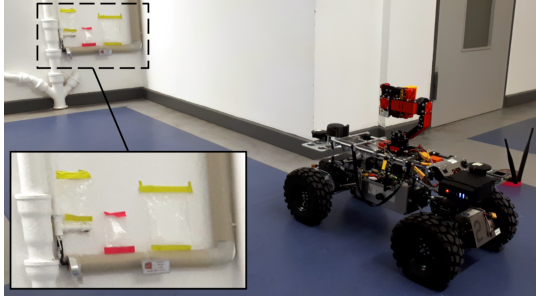
Fig. 1. Trial field used for the measurements. The robot (right) is scanning pipework (top left). Bags filled with 2.5 vol% methane are marked with yellow tape and placed on the pipework (inset left, inset right). A control bag filled with air is marked with red tape (inset middle).

Fig. 2. Assembled visual image (grayscale) and overlay of methane column density (red) as seen by the operator during the experiment.

software adaption while using no or only minimal hardware extensions.

II. MATERIALS AND METHODS

To evaluate the virtual gas camera under the aspects discussed in Sect. I, a suitable hardware, software, and trial field setup is devised in the following subsections.

A. Hardware Setup

The robot used for the evaluation consists of a four-wheeled frame previously presented in [8]. This system is controlled by a Hex Pixhawk Cube Orange autopilot, making it compatible with the ArduPilot open-source ecosystem and related ground control software. To this frame, an on-board computer with WiFi was added (UDOO x86 Ultra with AW-CB304NF). The OS is Ubuntu Desktop 22.04.3. A gimbal designed in-house was also added, which uses a BaseCam Electronics SimpleBGC 32-bit CAN_MCU / CAN_Driver / CAN_IMU system with T-Motor GB54-1 actuators. For methane column density measurements, a TDLAS device (LM1A06N-LFA by Tokyo Gas Engineering Solutions) is integrated into the gimbal. A Caddx Ratel camera is mounted next to the TDLAS device, monitoring its target area. The video of this camera is acquired by a LogiLink VG0030 digitizer.

B. Software Setup

The main function of the virtual gas camera is to perform a scan over the yaw and pitch angles of the gimbal while sampling the methane column density and simultaneously acquire a visual image. This data is then incorporated into an overlay showing the locations of increased methane presence. The software is written in Python 3. For interfacing with the gimbal controller, an open-source library is used [9]. For accessing the TDLAS device measurements, its proprietary protocol was analyzed, and an acquisition library was written.

The software is run and controlled wirelessly via an SSH terminal. It provides continuous live video to the operator for maneuvering and evaluation. When the measurement itself is started, the software first calculates the necessary parameters, such as the full yaw/pitch angles to match the current field of view, the step angles, and the portion of the camera frame

corresponding to the measured point/image area (subframe). It then starts sampling data for each angular position. For this, it first commands the gimbal to the desired position and waits for the video motion to settle. The methane column density is then acquired as well as the camera subframe. This process is afterwards repeated for the full field of view of the original livestream image.

After completion of the scan, the visual image is then assembled from the subframes. A full video frame in neutral position could also be used for the visual image. However, using subframes ensures that the measured column density values match the visual image exactly, even if there is drift. The results, including an overlay image of the column densities, are then stored, and made available via a network share. This allows for the results to be immediately reviewed from the ground control station.

All software needed for these operations is published open-source under [10]. For more details on software operation and communication the reader is referred there.

C. Trial Field

A trial field was devised to simulate a methane leak, see Fig. 1. The robot was placed 2.8 m in front of pipes installed on a wall. Two polyethylene zip bags 18 cm x 23 cm and 12 cm x 17 cm in size were filled with a gas containing 2.5 vol% methane (Dräger 6811131) and marked at the edges with yellow tape. The bags were placed on top of the pipes. A third bag was filled with air as control for possible false positives from bag-beam interaction, marked with red tape, and placed similarly. Its size was 9 cm x 16 cm. The thickness of the small bags in the direction of the beam was ca. 2.5 cm and for the large bag it was ca. 5 cm.

III. RESULTS AND DISCUSSION

A. Results

A measurement was performed with $25 \cdot 25 = 625$ subframes. The resulting acquisition time was seven minutes. For the column density at each sample location, five measurements were taken, and the median value used. Fig. 2 shows an overlay of the methane column density in red onto a grayscale image assembled from subframes.

With regards to the visual image, a satisfactory quality was achieved. It allows the operator to easily identify objects,
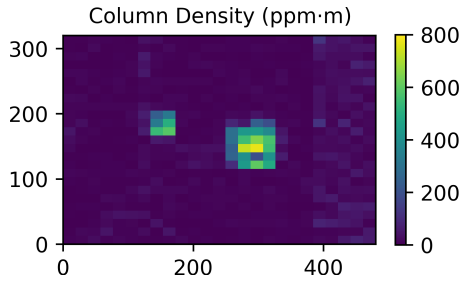
Fig. 3. Plot of only the methane column density data of the experiment shown in Fig. 2. Axis coordinates are in full camera frame pixels. Column density data consists of $25 \cdot 25$ samples. Both methane bags can be clearly identified.

such as the pipework. However, in some areas stepped edges are seen, e.g. on the top left and top right pipe edges. These probably stem from angle errors still present at the point in time when the subframe was acquired.

With regards to the column density overlay, the two methane-filled bags on the left and right are clearly detected, while the control bag with air does not show any response. The noise background is generally low. Some noise is visible on the righthand side, where the measurement beam hits the wall at an oblique incidence.

To better evaluate the raw signal quality, a direct column density plot was created after the experiments, see Fig. 3. It can be seen that there is no signal from the control bag even in the raw data. The increased noise on the right-hand side can be more clearly seen to be confined to the right-hand oblique wall. This data also allows to give absolute column densities: 588 ppm·m for the small, and 773 ppm·m for the large bag.

B. Discussion

One aspect that stands out is that the virtual gas camera takes a significantly longer time to acquire an image than an actual gas camera. Gas cameras usually acquire multiple frames with hundreds-of-pixel resolution in a single second [11]. The presented setup acquires $25 \cdot 25$ data in seven minutes, leading to an average acquisition time per location of 672 ms. Of this, 500 ms are consumed by the five measurements taken by the TDLAS device in 100 ms intervals. The rest is gimbal travel and settle time. This could be improved by only acquiring a single sample per location, bringing the theoretical acquisition time down to 2.8 minutes. However, this can be expected to increase noise. The threshold for waiting for the video motion to settle could also be decreased. Yet, the stepped edges present in Fig. 2 suggest that this is already at a sensible limit. Additionally, the setup as-is already demonstrates a 33 % improvement over the 1 s scan sample acquisition time demonstrated previously with pan/tilt units [2].

Another aspect to note is that the presented setup samples the methane data in the middle of the subframe with a limited beam opening angle (< 8.5 mrad). Thus, if the angular subframe size is large due to a limited number of subframes, the measurement beam might miss a source within the subframe. This could be mitigated by taking multiple measurements within the subframe at the expense of acquisition time.

Regarding the main question of this paper, the results show that the virtual gas camera setup can detect methane leaks similar to an actual gas camera. All placed sources can be clearly identified and can be correlated with their location using the assembled visual image. The data is immediately available to the operator as soon as acquisition is finished. The measurement was furthermore performed fully wirelessly. This demonstrates that the presented prototype of the virtual gas camera can fulfill its main task successfully.

IV. Conclusion and Outlook

The results have shown that the addition of a virtual gas camera to a TDLAS setup is possible and can be used to perform visual leak detection. The main drawback identified in comparison to conventional gas cameras is acquisition time. It should be noted that this can likely be improved, see Sect. III-B. Furthermore, the virtual gas camera is an addition to a system that can perform tasks a gas camera alone cannot, and can thus be seen as an additional, secondary operation mode. A possible application of this could be to generate a quick visual overview when the robot first arrives at a suspected location. It should also be stressed, that the virtual gas camera comes at little to no additional hardware expense for a typical TDLAS tomography system.

In the future, the concept could be extended by more fundamental changes than the ones discussed in Sect. III-B. Continuous rotation and sampling in combination with a camera able to acquire images at high framerates would remove the need for video settling times during acquisition and therefore cut down on measurement time significantly.

References

[1] S. Soldan, G. Bonow, and A. Kroll, "RoboGasInspector - A Mobile Robotic System for Remote Leak Sensing and Localization in Large Industrial Environments," *IFAC Proc. Vol.*, vol. 45, no. 8, pp. 33–38, 2012.

[2] V. M. H. Bennetts *et al.*, "Towards real-world gas distribution mapping and leak localization using a mobile robot with 3D and remote gas sensing capabilities," in *2013 IEEE Int. Conf. Robotics and Automation*, 2013, pp. 2335–2340.

[3] Y. Zeng and J. Morris, "Detection limits of optical gas imagers as a function of temperature differential and distance," *J. Air Waste Manage. Assoc.*, vol. 69, no. 3, pp. 351–361, 2019.

[4] N. Hagen, "Survey of autonomous gas leak detection and quantification with snapshot infrared spectral imaging," *J. Opt.*, vol. 22, no. 10, p. 103001, 2020.

[5] K. Uehara and H. Tai, "Remote detection of methane with a 1.66-um diode laser," *Appl. Optics*, vol. 31, no. 6, pp. 809–814, 1992.

[6] V. H. Bennetts *et al.*, "Robot assisted gas tomography — Localizing methane leaks in outdoor environments," in *2014 IEEE Int. Conf. Robotics and Automation*, 2014, pp. 6362–6367.

[7] P. P. Neumann *et al.*, "Aerial-based gas tomography – from single beams to complex gas distributions," *Eur. J. Remote Sensing*, vol. 52, no. sup3, pp. 2–16, 2019.

[8] P. P. Neumann *et al.*, "Towards autonomous NDT inspection: Setup and validation of an indoor localization system," in *39th Danubia-Adria Symp. Adv. Exp. Mechanics*, 2023, pp. 88–89.

[9] M. Maier. Robot cameraman simplebgc library. [Online]. Available: https://github.com/maiermic/robot-cameraman/tree/master/simplebgc

[10] H. Lohrke. Virtual gas camera software repository. [Online]. Available: https://github.com/BAMresearch/virtual-gas-camera

[11] Teledyne FLIR. Gx320 14.5° datasheet. [Online]. Available: https://support.flir.com/DsDownload/Assets/10401-0101-en-US.html